Cancer Immunology, Immunotherapy (2019) 68:305–318
https://doi.org/10.1007/s00262-018-2278-x

ORIGINAL ARTICLE

Tumor-infiltrating immune cell subpopulations and programmed death ligand 1 (PD-L1) expression associated with clinicopathological and prognostic parameters in ependymoma

Soo Jeong Nam[1] · Young-Hoon Kim[2] · Ji Eun Park[3] · Young-shin Ra[2] · Shin Kwang Khang[1] · Young Hyun Cho[2] · Jeong Hoon Kim[2] · Chang Ohk Sung[1]

Received: 18 April 2018 / Accepted: 21 November 2018 / Published online: 27 November 2018
© Springer-Verlag GmbH Germany, part of Springer Nature 2018

Abstract

Ependymomas are biologically and clinically heterogeneous tumors of the central nervous system that have variable clinical outcomes. The status of the tumor immune microenvironment in ependymoma remains unclear. Immune cell subsets and programmed death ligand 1 (PD-L1) expression were measured in 178 classical ependymoma cases by immunohistochemistry using monoclonal antibodies that recognized tumor-infiltrating lymphocyte subsets (TILs; CD3, CD4, CD8, FOXP3, and CD20), tumor-associated macrophages (TAMs; CD68, CD163, AIF1), indoleamine 2,3-dioxygenase (IDO)+ cells and PD-L1-expressing tumor cells. Increases in CD3+ and CD8+ cell numbers were associated with a prolonged PFS. In contrast, increased numbers of FOXP3+ and CD68+ cells and a ratio of CD163/AIF1+ cells were significantly associated with a shorter PFS. An increase in the IDO+ cell number was associated with a significantly longer PFS. To consider the quantities of TILs, TAMs, and IDO+ cells together, the cases were clustered into 2 immune cell subgroups using a k-means clustering analysis. Immune cell subgroup A, which was defined by high CD3+, low CD68+ and high IDO+ cell counts, predicted a favorable PFS compared to subgroup B by univariate and multivariate analyses. We found six ependymoma cases expressing PD-L1. All these cases were supratentorial ependymoma, RELA fusion-positive (ST-RELA). PD-L1 expression showed no prognostic significance. This study showed that the analysis of tumor-infiltrating immune cells could aid in predicting the prognosis of ependymoma patients and in determining therapeutic strategies to target the tumor microenvironment. PD-L1 expression in the ST-RELA subgroup suggests that this marker has a potential added value for future immunotherapy treatments.

Keywords Immune microenvironment · Tumor-infiltrating lymphocytes · Tumor-associated macrophages · Indoleamine 2,3-dioxygenase · Ependymoma · Programmed death ligand 1

Soo Jeong Nam and Chang Ohk Sung are corresponding authors.

Electronic supplementary material The online version of this article (https://doi.org/10.1007/s00262-018-2278-x) contains supplementary material, which is available to authorized users.

✉ Soo Jeong Nam
soojeong_nam@amc.seoul.kr

✉ Chang Ohk Sung
co.sung@amc.seoul.kr

[1] Department of Pathology, Asan Medical Center, Seoul, South Korea

[2] Department of Neurosurgery, Asan Medical Center, Seoul, South Korea

[3] Department of Radiology, Asan Medical Center, Seoul, South Korea

Abbreviations

AIF1	Allograft inflammatory factor 1
CNS	Central nervous system
GTS	Gross total resection
ICC	Intraclass correlation coefficient
KPS	Karnofsky Performance Scale
NF2	Neurofibromatosis type 2
PF	Posterior fossa
PF-A	Posterior fossa ependymoma, group A
PF-B	Posterior fossa ependymoma, group B
SP	Spinal cord
ST	Supratentorial
ST-RELA	Supratentorial ependymoma, RELA fusion-positive
STR	Subtotal resection
TAMs	Tumor-associated macrophages/microglia

Introduction

Ependymomas are primary tumors of the central nervous system (CNS) that morphologically resemble the ependymal cells lining the ventricles of the CNS. Ependymoma is a histologically defined intrinsic tumor that involves the three major anatomic compartments (i.e., supratentorial region; ST, posterior fossa; PF, and spinal cord; SP) of the CNS and affects both children and adults.

The 10-year overall survival (OS) of ependymoma patients is approximately 66% for pediatric patients and ranges from 70 to 89% for adult patients. The prognostic influence of clinical factors, including age, tumor site and extent of resection, has been well established in previous studies on ependymoma [1–3].

The ependymoma grading system is based on that of the World Health Organization (WHO). However, no association between grade and biological behavior or survival has been definitively established [4]. Several publications have discussed the challenges that are posed by the existing criteria, which use morphological features to determine the grade of an ependymoma; this discussion has led to an ongoing debate regarding the significance of the ependymoma grade in predicting the prognosis of the patient [5].

Recently, immunotherapy targeting programmed death-1 (PD-1)/programmed death ligand 1 (PD-L1) has shown clinical benefits in glioma patients [6]. In addition, tumor vaccines against glioma are being developed for immunotherapy, and several agents that specifically target pathways that mediate the interaction between neoplastic and tumor microenvironment cells have entered clinical trials [7, 8]. In ependymoma, exhausted T-cells associated with PD-L1/PD-1 interaction were identified in a subset of supratentorial ependymoma, RELA fusion-positive (ST-RELA), which suggested a benefit of PD-1 inhibitor therapy [9].

The importance of the tumor microenvironment has been increasingly recognized, and the complexity of the interaction between tumor cells and tumor microenvironment cells is becoming clear [10]. Previous studies have reported the prognostic role of tumor-infiltrating lymphocytes (TILs) in gliomas. In a study of glioblastoma, high levels of CD4+ T cells and low levels of CD8+ T cells were associated with unfavorable prognosis [11]. Consistently, in other studies on glioblastoma, increased CD3+ and CD8+ T cell infiltration was associated with prolonged survival [12, 13]. However, in other studies of glioblastoma patients, a higher density of CD8+ T cells showed no significant relationship with survival. In contrast, patients with a higher density of Foxp3+ T cells showed relatively lower survival rates in the same study [14].

Generally, tumor-associated macrophages/microglia (TAMs) play a major role in the creation of a tumor microenvironment that promotes tumor progression. For glioma, many studies have revealed that TAMs and M2-type macrophages exert glioma-supportive effects through reduced antitumor functions, increased expression of immunosuppressive mediators [15], and nonimmune tumor promotion through the expression of trophic- and invasion-facilitating substances [16, 17].

Indoleamine 2,3-dioxygenase (IDO) is a tryptophan-catabolizing enzyme produced by myeloid, stromal, and epithelial cells [18]. IDO exerts its immunosuppressive effects by depleting local tryptophan stores and producing kynurenine, a tryptophan metabolite [19]. IDO contributed to tumor progression and metastasis in vivo, and increased IDO expression was associated with poor prognosis in patients with solid tumors and glioblastoma [20, 21]. In IDO-deficient mouse glioma models, IDO-deficient tumors provide a survival advantage against IDO-competent tumors [22]. Other reports suggested a critical role for IDO–Treg interaction-mediated immunosuppression in both mouse glioma models [23] and adult primary glioblastoma cases [24].

Only one previous study reported the prognostic significance of tumor-infiltrating immune cells in ependymoma. This study showed that infiltration of CD4 + T cells and allograft inflammatory factor 1 (AIF1) + TAMs was decreased in the patients who subsequently experienced recurrence. However, there was no significant difference in HLA-DR+ cells, CD45+ lymphocytes, CD8+ T cells, CD20+ B cells and CD68+ TMAs between the nonrecurrent and recurrent groups of ependymoma patients [25].

Therefore, little is known about the immune microenvironment and its clinicopathological characteristics in ependymoma. Moreover, there has been no integrated analysis of various tumor-infiltrating immune cells, including TILs, TAMs, and IDO, in ependymoma. Thus, the present study was intended to comprehensively investigate the immunological microenvironment. Using an automatic evaluation system for immunohistochemistry (IHC), we characterized the subpopulations of TILs, TAMs, and IDO+ cells, examined the expression of PD-L1 in formalin-fixed paraffin-embedded ependymoma tissues and elucidated the prognostic values of these factors in ependymomas.

Materials and methods

Patients

A total of 178 patients who were diagnosed with WHO grade II or III ependymomas at Asan Medical Center between 1996 and 2012 were included in this study. The neuropathologists (S.J. Nam, S.K. Khang, and C.O. Sung) reviewed the pathological materials according to current WHO criteria. The clinical data were obtained from the

medical records and reviewed by a neuropathologist, neuroradiologist, and neurosurgeon (S.J. Nam, J.E. Park and Y.H. Kim, respectively). The follow-up periods ranged from 0.77 to 240.97 months, and the mean was 57.62 months. At the time of review, 16 patients (13.1%) had died, and 26 patients (19.0%) had been lost to follow-up.

Immunohistochemistry

Core tissues that were 2 mm in diameter were obtained from the representative formalin-fixed paraffin-embedded tissue blocks that were obtained from patient tumor samples, and tissue microarrays were manufactured for further immunohistochemical analysis. Two different fields of the intratumoral area, excluding necrotic or squeezed areas, were taken from the original block to manufacture tissue microarrays. CD3, CD4, and CD8 were used as T cell markers. CD20 was used as a B cell marker. CD68 and AIF1 were used as TAM markers, CD163 was used as an M2 TAM marker, and FOXP3 was used as a Treg marker. IDO highlighted the IDO-producing dendritic cells or macrophages. PD-L1 immunostaining was used to detect PD-L1 expression in the tumor cell membrane. L1CAM immunostaining was used to identify L1CAM-expressing ST ependymoma, suggesting ST-RELA.

Immunostaining for CD3 (polyclonal, diluted at 1:100, Agilent Technologies, Inc., Santa Clara, CA), CD4 (SP35, diluted at 1:16, Ventana Medical Systems, Inc., Tucson, AZ, USA), CD8 (C8/144B, diluted at 1:400, Agilent Technologies, Inc., Santa Clara, CA), CD20 (L26, diluted at 1:400, Agilent Technologies, Inc.), CD68 (KP-1, diluted at 1:2000, Agilent Technologies, Inc., Santa Clara, CA), CD163 (10D6, diluted at 1:400, Novocastra, Newcastle Upon Tyne, UK), FOXP3 (236A/E7, diluted at 1:100, Abcam, Cambridge, UK), AIF1 (ABN67, diluted at 1:1000, Millipore, Billerica, MA, USA), IDO (1F8.2; diluted at 1:250, Millipore, Billerica, MA, USA), PD-L1 (SP263, ready-to-use, Ventana Medical Systems, Inc., Tucson, AZ, USA and E1L3N, Cell Signaling Technology, Inc., Danvers, MA, USA) and L1CAM (L4543, 1:2000, Sigma-Aldrich, MO, USA) were performed using a BenchMark XT Autostainer (Ventana Medical Systems, Inc., Tucson, AZ, USA). Immunostaining was performed, according to the manufacturer's protocols.

Automated quantification of TILs, TAMs, and IDO+ cells by image analysis

To perform an unbiased analysis of tumor-infiltrating immune cells and to obtain objective and reproducible data, virtual microscopy and automatic enumeration were performed using an image analyzer. All of the immunostained slides were subjected to virtual microscope scanning under high-power magnification using a Panoramic 250 Flash III (3DHISTECH Ltd, Budapest, Hungary). For the enumeration of immune cells, representative fields of the intratumoral area were captured from virtual microscopic images. The numbers of CD3+, CD4+, CD8+, FOXP3+, CD20+, CD68+, CD163+, AIF1+, and IDO+ cells were counted using ImageJ software (National Institutes of Health, Bethesda, MD, USA), as previously described [26]. The numbers of positive cells per unit area (1 mm^2) were calculated from the obtained values and used for further statistical analysis.

To validate the representativeness of the TMA for evaluating tumor-infiltrating immune cells, we evaluated a series of whole sections from reference cases and compared the counts in these tissues to the counts from the TMA. As a reference, 10% (18 cases) of cases were selected to be evenly distributed. The agreement between the immune cell counts obtained from the TMA and from the whole section was assessed using the intraclass correlation coefficient (ICC). The ICC value showed significant excellent agreement for most measurements ($ICC > 0.8$ and $P < 0.001$), and some ICCs were greater than 0.9 (for CD68, CD163 and AIF1). The ICCs for whole sections and TMA were as follows: 0.896 for CD3, 0.819 for CD4, 0.854 for CD8, 0.944 for CD68, 0.948 for CD163 and 0.940 for AIF1. In addition, the ICCs of FOXP3+ and IDO+ cells were 0.765 and 0.797 ($P = 0.002$ and 0.001, respectively). By contrast, the ICC value for CD20 was 0.352 ($P = 0.183$). Consequently, TMA could be considered sufficiently representative for immune cell evaluation, except for CD20+ cells, in this study.

PD-L1 and L1CAM were evaluated nonquantitatively. Cases expressing PD-L1 diffusely or focally were restained in whole section. Diffuse membranous expression of more than 10% of tumor cells for PD-L1 and diffuse strong cytoplasmic expression of L1CAM were regarded as positive. For PD-L1, the histologically defined intratumoral area, excluding necrotic or inflammatory cells such as macrophages, was evaluated.

Statistical analysis

All statistical analyses were performed with SPSS 22 (IBM Corp., New York, NY, USA). A nonparametric Wilcoxon rank-sum test was performed to assess the differences in the numbers and ratios of immune cells according to the clinicopathological variables. For the survival analysis, we fitted survival curves to a Kaplan–Meier model after dichotomizing the cases into two groups using Cutoff Finder (http://molpath.charite.de/cutoff/index.jsp) [27]. The values that were defined as the points with the most significant split between groups, including PFS and OS, were selected as the cutoffs using a log-rank test. This approach resulted in the following cutoff values: 0.4849 for CD3, 28 for CD4, 13.88 for CD8, 0.7662 for CD4/CD8, 0.5066 for FOXP3, 16.59 for

CD20, 93.62 for CD68, 69.73 for CD163, 1.007 for CD163/CD68, 798.3 for AIF1, 0.265 for CD163/AIF1 and 4.201 for IDO (cell counts/mm^2). In addition, univariate and multivariate survival analyses were performed using Cox proportional hazards models. Two-sided P values <0.05 were considered statistically significant for all analyses. To incorporate the analysis of various immune cells, the cases were clustered into 2 immune cell subgroups according to the status of CD3+ T-cells, CD68+ macrophages and IDO+ cells using k-means clustering. Kaplan–Meier survival analysis and univariate and multivariate Cox proportional hazards models were also performed for immune cell subgroups.

Results

Clinicopathological characteristics of patients with ependymoma

The clinicopathological characteristics of patients with ependymoma are summarized in Supplementary Table S1. The male-to-female ratio was 1.2:1, and patient age ranged from 0 to 73 (mean of 24.2 and median of 16) years. The Karnofsky Performance Scale (KPS) ranged from 0 to 90 (mean 73.79 and median 80). The majority of patients received a gross total resection (GTS; 81.1%, 107/132). The prevalence of WHO grade II ependymomas was estimated as 78.1% (139/178). Many patients received only surgical treatment (59.5%, 78/131). Other patients received adjuvant radiotherapy (32.8%, 43/131) and chemotherapy (14.6%, 19/130). The prevalence of ST ependymomas was estimated as 27.5% (49/178). PF ependymomas and SP ependymomas were observed in 43.3% (77/178) and 29.2% (52/178) of cases, respectively.

Histopathologically, high-grade features from the WHO classification of ependymomas [4], including microvascular proliferation (22.5%, 40/178), necrosis (46.1%, 82/178), cytological atypia (74.7%, 133/178) and increased mitotic activity (≥ 5; 74.2%, 132/178), were evaluated. Cytologic atypia was defined when tumor cells exhibited a high nuclear-to-cytoplasmic ratio across more than 25% of the tumor. Cases with a high nuclear-to-cytoplasmic ratio usually show hyperchromatic nuclei. High cell density nodules were recorded as proliferating nodules (16.3%, 29/178). L1CAM was expressed in 9.8% (16/170) of ependymoma cases. Most of the L1CAM-positive cases were ST ependymoma (93.8%, 15/16).

Kaplan–Meier survival analysis was performed for clinicopathological features. Several variables were associated with worse PFS and OS, including younger age (<20; $P<0.001$, both), low KPS score (<80; $P=0.016$ and 0.037), subtotal resection (STR; $P=0.002$ and $P<0.001$), adjuvant radiotherapy ($P<0.001$ and $P=0.004$), adjuvant chemotherapy ($P<0.001$, both), high WHO grade (WHO grade III; $P<0.001$ and $P=0.389$), intracranial location ($P=0.001$ and 0.009), presence of microvascular proliferation ($P=0.016$ and 0.088), presence of proliferating nodule ($P<0.001$ and $P=0.013$), presence of cytologic atypia ($P=0.036$ and 0.629) and high mitotic count (≥ 5; $P<0.001$ and $P=0.001$) (data not shown). The results of univariate Cox analysis are summarized in Supplementary Table S2.

Quantitative analysis of tumor-infiltrating immune cells in ependymoma

The distribution patterns of immune cells varied depending on the type of immune cell. The distribution pattern of lymphocytes was relatively even in both the perivascular and intratumoral areas. In contrast, macrophages and IDO+ cells showed a more concentrated distribution in the perivascular area.

Lymphocytes staining for CD3, CD8, and CD20 were immunostained in the membrane and/or cytoplasm of small lymphocytes (Fig. 1a, c, e). FOXP3+ cells were shown to have distinct nuclear patterns (Fig. 1d). CD4 was immunostained in the cytoplasm of small lymphocytes and in some histiocytes/dendritic cells (Fig. 1b). The CD4 staining intensity was strong in small lymphocytes and relatively weak in histiocytes/dendritic cells. To count CD4+ lymphocytes, an intensity criterion for CD4 to dichotomize small lymphocytes from histiocytes/dendritic cells was applied. The mean numbers of CD3+, CD4+, CD8+, FOXP3+ and CD20+ cells per 1 mm^2 were 32.1 (range 0-573.4, median 8.9), 29.7 (range 0–413.6, median 6.8), 24.9 (range 0–416.8, median 5.9), 6.7 (range 0–321.3, median 0) and 5.5 (range 0–210.7, median 0). The mean ratio of CD4/CD8 + cells was 4.9 (range 0–65.3, median 0.8).

CD68, CD163 and AIF1 were immunostained with a cytoplasmic and/or membranous pattern in cells presumed as macrophages based on morphology, as shown in Fig. 1f, g, h. The mean number of tumor-infiltrating CD68+ cells, CD163+ and AIF1+ cells in ependymoma was 141.0 (range 0–1107.8, median 54.3), 301.8 (range 0–1757.0, median 192.1) and 815.53 (range 56–1758, median 804.76) per 1 mm^2, respectively. The mean ratio of CD163/CD68+ cells and CD163/AIF1+ cells was estimated to be 10.4 (range 0–281.4, median 2.5) and 0.47 (range 0–7.65, median 0.36).

IDO was expressed in the cytoplasm of tumor-infiltrating immune cells, which were primarily suspected to be macrophages, dendritic cells or plasmacytoid dendritic cells based on their morphology (Fig. 1i). Overall, the mean number of IDO+ cells per 1 mm^2 was 6.2 (range 0–154.7, median 0.9).

Overall, the number of CD3+ cells showed a significant positive correlation with the numbers of CD4+, CD8+ and CD68+ cells ($R=0.336$, 0.705 and 0.436; $P<0.001$ for

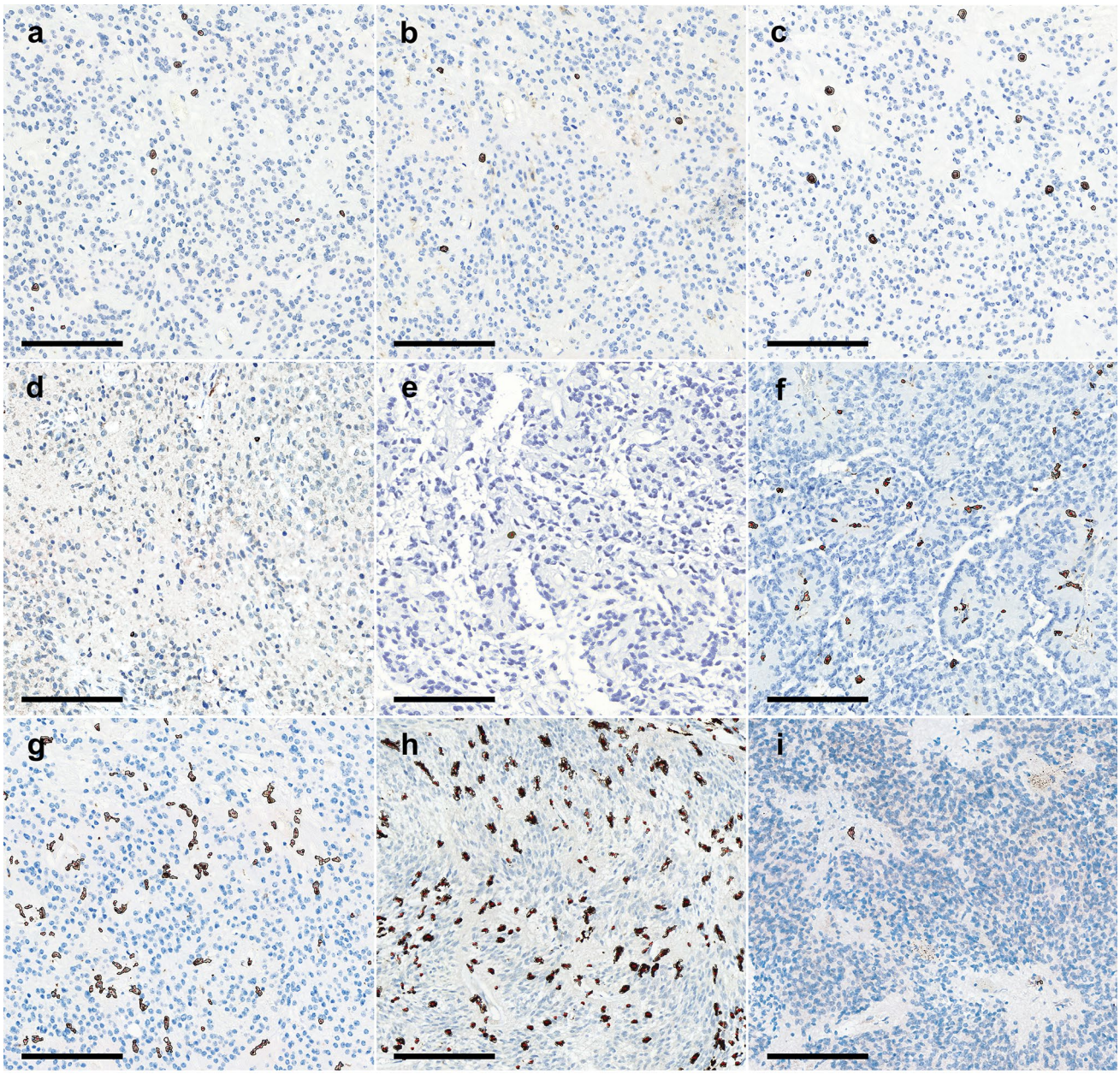

Fig. 1 Representative images of the automatic enumeration of tumor-infiltrating immune cells. Representative images from the automated enumeration of tumor-infiltrating CD3+, CD4+, CD8+, FOXP3+, CD20+, CD68+, CD163+, AIF1+, and IDO+ cells. Images were captured by virtual microscopy and submitted to an image analyzer, which delineated the positive cells by thin black lines. CD3, CD8, FOXP3, and CD20 staining was localized in small lymphoid cells. CD4 was found on either small lymphoid cells or histiocytes. CD68, CD163, and AIF1 were localized in a granular cytoplasmic pattern by macrophages. IDO was localized in a granular cytoplasmic pattern by what were suspected to be macrophages, dendritic cells and/or small plasmacytoid dendritic cells. The counts of CD3+ (**a**), CD4+ (**b**), CD8+ (**c**), FOXP3+ (**d**), CD20+ (**e**), CD68+ (**f**), CD163+ (**g**), AIF1+(**h**) and IDO+ cells (i) in this case were 12, 6, 12, 2, 1, 43, 77, 206, and 2 per unit area (1 mm^2), respectively. (Scale bar, 100 µm, in all images)

all; Supplementary Fig. S1), but not with the numbers of FOXP3+ or CD20+ cells (Supplementary Fig. S1). The number of CD68+ cells also showed a significant positive correlation with the number of CD163+ cells ($R = 0.488$; $P < 0.001$; Supplementary Fig. S1). The number of AIF1+ cells showed a significant positive correlation with the number of CD68+ cells ($R = 0.278$; $P = 0.001$; Supplementary Fig. S1). The number of IDO+ cells was positively correlated with the number of FOXP3+ cells ($R = 0.203$; $P = 0.008$; Supplementary Fig. S1).

Relationships between clinicopathological features and the number of tumor-infiltrating immune cells in ependymoma samples

The associations between the clinicopathological features and the numbers of tumor-infiltrating immune cells are summarized in Supplementary Table S1. Briefly, the number of CD3+ cells was decreased in cases that showed microvascular proliferation ($P=0.008$). A greater number of CD4+ cells was frequently observed in younger patients (age <20; $P=0.001$ and 0.07, respectively), WHO grade III ependymoma ($P=0.002$), profound nuclear atypia ($P<0.001$) and L1CAM-positive ependymoma ($P=0.021$). The counts of CD8+ cells were decreased in cases with microvascular proliferation ($P=0.008$) and increased in cases with higher mitotic activity (mitotic count ≥5; $P<0.001$). Increased FOXP3+ cell counts were observed in cases with profound nuclear atypia ($P=0.022$). Increased numbers of CD68+ cells were frequently observed in young patients (age <20; $P=0.006$), cases of WHO grade III ependymomas ($P<0.001$), patients who received adjuvant radiotherapy and chemotherapy ($P=0.047$ and 0.010, respectively), cases with profound nuclear atypia ($P=0.018$), cases with increased mitotic activity (mitotic count ≥5; $P=0.040$) and cases of L1CAM-positive ependymomas ($P=0.003$). CD163 + cell counts were associated with WHO grade III ependymomas ($P=0.005$), necrosis ($P=0.009$), profound nuclear atypia ($P<0.001$) and L1CAM-positive ependymomas ($P=0.002$). The ratio of CD163/CD68+ cells was lower in WHO grade III ependymomas ($P<0.001$) and cases with increased mitotic activity (mitotic count ≥5; $P=0.007$). The number of AIF1+ cells decreased in cases with microvascular proliferation ($P=0.003$) or necrosis ($P=0.008$) and increased in cases with higher mitotic activity (mitotic count ≥5; $P=0.002$) and L1CAM-negative ependymoma ($P=0.047$). The increased ratio of CD163/AIF1+ cells was frequently observed in younger patients (age <20; $P=0.007$), patients who received adjuvant radiotherapy ($P=0.011$), WHO grade III ependymoma ($P=0.001$), cases with microvascular proliferation ($P=0.001$), necrosis ($P<0.001$), profound nuclear atypia (P<0.001), cases with higher mitotic activity (mitotic count ≥5; P=0.003) and L1CAM-positive ependymoma ($P=0.041$). The number of IDO+ cells was also decreased in cases with nodular growth ($P=0.002$) and increased mitotic activity (mitotic count ≥5; $P=0.024$). Otherwise, there were no significant associations between the tumor-infiltrating immune cell status and other clinicopathological features.

The number of tumor-infiltrating immune cells and ependymoma patient survival

A total of 137 patients with ependymoma were classified into two groups according to the quantity and status of the tumor-infiltrating immune cells, as described in the Materials and Methods section, and studied for survival analysis. In the Kaplan–Meier analysis, patients with increased CD3 and CD8+ cell counts exhibited better PFS ($P=0.019$ and 0.007, respectively) (Fig. 2a, c) and tended to exhibit prolonged OS ($P=0.198$ and 0.063, respectively) (Supplementary Fig. S2a and c). In contrast, a high ratio of CD4/CD8+ cells and an increased number of FOXP3+ cells were associated with worse PFS ($P=0.010$ and 0.022, respectively) (Fig. 2d, e). Patients with high CD68+ cell counts and a high ratio of CD163/AIF1+ cells also showed a significantly poor PFS ($P<0.001$ and $P=0.014$) (Fig. 2g, k). Increased IDO+ cell counts were associated with a prolonged PFS ($P=0.012$) (Fig. 2l). Increased CD4+ cells and CD163+ cells and decreased AIF1+ cells tended to be related to shortened PFS ($P=0.053$, 0.064 and 0.066, respectively) (Fig. 2b, h, j). An increased number of CD20+ cells and an increased ratio of CD163/CD68 + cells tended to be related to prolonged PFS and OS (CD20, $P=0.060$ and 0.063, respectively; CD163/CD68, $P=0.067$ and 0.070, respectively) (Fig. 2f, i and Supplementary Fig. S2f and i).

The prognostic tendencies of the immune cell expression characteristics were maintained in the subgroups of ependymoma patients who were classified according to their WHO grade, age and site of tumor (Supplementary Fig. S3 and S4). In WHO grade II ependymoma patients, the cases with higher numbers of CD3 and CD8+ cells exhibited better PFS ($P=0.057$ and 0.013, respectively) (Supplementary Fig. S3a and c). A high ratio of CD4/CD8+ cells and an increased number of FOXP3+ cells were associated with worse PFS ($P=0.012$ and 0.021, respectively) (Supplementary Fig. S3d and e). Patients with high CD68+ cell counts also showed a significantly worse PFS ($P<0.001$) (Supplementary Fig. S3g). Increased IDO+ cell counts were associated with a prolonged PFS ($P=0.019$) (Supplementary Fig. S3l). When the analysis was stratified by pediatric and adult patients, these trends were maintained (Supplementary Fig. S4). Among these trends, a high ratio of CD4/CD8+ cells was associated with a significantly worse PFS in pediatric ependymoma patients ($P=0.028$). Adult patients with increased FOXP3+ and CD68+ cell counts also showed a significantly poor PFS ($P=0.040$ and $P<0.001$, respectively). Otherwise, although the trends of the survival curve were maintained, there was no statistically significant relationship between any cell profile and patient survival. These tendencies were also maintained when patients were classified based on their primary tumor site. However, statistical significance was preserved only in PF ependymoma patients (CD3, $P=0.029$; CD8, $P=0.038$; CD4/CD8, $P=0.005$; FOXP3, $P=0.038$; CD68, $P=0.002$; and IDO, $P=0.022$) (Supplementary Fig. S4).

To incorporate the quantities of TILs, TAMs, and IDO+ cells, cases were clustered into two immune cell subgroups using a k-means clustering analysis. Immune cell subgroup A

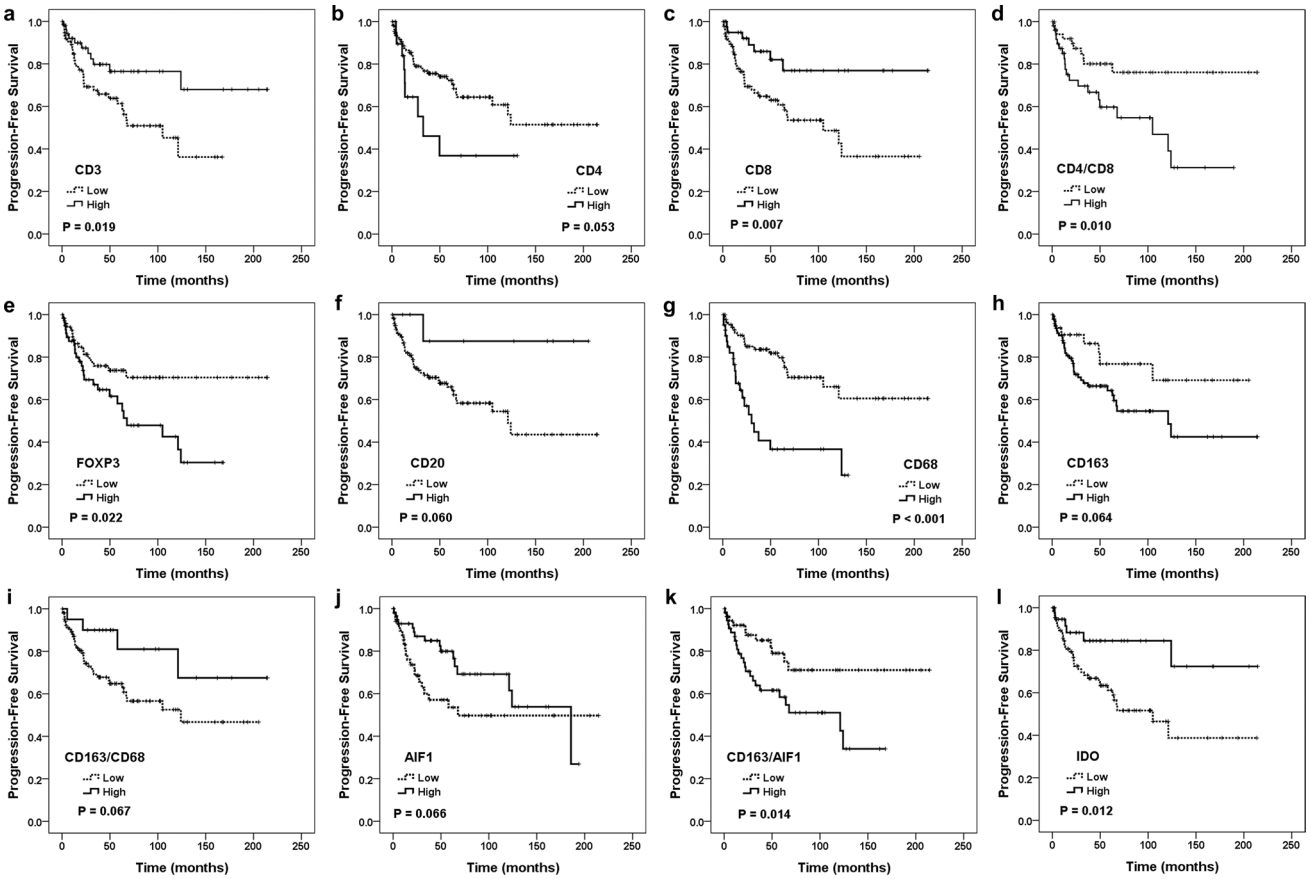

Fig. 2 Survival analysis according to the numbers of tumor-infiltrating immune cells. PFS of ependymoma patients was evaluated according to the number of tumor-infiltrating CD3+ (**a**), CD4+ (**b**), CD8+ (**c**), FOXP3+ (**e**), CD20+ (**f**), CD68+ (**g**), CD163+ (**h**), AIF1+ (**j**) and IDO+cells (**l**), and the ratios of CD4/CD8+ (**d**), CD163/CD68+ (**i**) and CD163/AIF1+cells (**k**). Kaplan–Meier curves for PFS are illustrated with the P values from the log-rank test

was defined by having high CD3+ and IDO+ cell counts and low CD68+ cell counts, and subgroup B had the opposite profile ($P=0.043$, 0.002 and <0.001, respectively). The clinicopathological features and immune cell counts of the immune cell subgroups are summarized in Table 1. The patient characteristics of subgroup A were older age and WHO grade II and SP ependymomas, whereas subgroup B were younger age and WHO grade III and intracranial ependymomas (Table 1). Subgroup A patients exhibited a statistically significantly favorable PFS compared to the subgroup B patients ($P<0.001$) (Fig. 3a). The significant difference in survival was maintained even when cases were stratified according to their WHO grade, age and primary tumor site (Fig. 3).

Independent prognostic implications of tumor-infiltrating immune cells in ependymoma patients

To further determine the prognostic implications of CD3+, CD4+, and CD8+ T cells; FOXP3+ regulatory T cells; CD68+ CD163+ and AIF1+ TAMs; and IDO+ cells in ependymoma, we performed a univariate and multivariate survival analysis using the Cox proportional hazards model. As summarized in Supplementary Table S2, the univariate Cox analysis revealed that the numbers of CD3+, CD8+, FOXP3+, CD68+, and IDO+ cells and the ratio of CD4+/CD8+ cells and CD163/AIF1+ cells predicted the PFS. A multivariate Cox regression analysis that integrated clinicopathological risk factors, including age, KPS score, extent of resection, adjuvant chemotherapy, adjuvant radiotherapy, WHO grade, and tumor site, and high-grade histopathological features, including microvascular proliferation, nodular proliferation, cytological atypia, increased mitotic activity and immune cell counts, was used to reveal prognostic factors among those patients who were identified in the univariate Cox regression analysis. In the multivariate analysis, low CD3+, high FOXP3+, high CD68+ and low IDO+ cell numbers and a high ratio of CD163/AIF1+ cells independently predicted poor a PFS ($P=0.072$, 0.008, 0.004, 0.012 and 0.041,

Table 1 Comparisons of the clinicopathologic features and immune cell counts according to their immune cell subgroup in ependymoma patients

Variables	Immune cell subgroup A ($N=49$)	Immune cell subgroup B (N = 77)	P
Age[b] (N (%))			
< 20	12 (24.5)	36 (46.8)	0.012
≥ 20	37 (75.5)	41 (53.2)	
WHO grade[b] [N (%)]			
II	49 (100)	64 (83.1)	0.002
III	0 (0)	13 (16.9)	
Site[c] [N (%)]			
ST	4 (8.2)	23 (29.9)	0.001
PF	19 (38.8)	35 (45.5)	
SP	26 (53.1)	19 (24.7)	
CD3[ad] (cell counts/mm^2)			
Mean ± SD	43.26 ± 86.75	20.14 ± 38.28	0.043
CD4[ad] (cell counts/mm^2)			
Mean ± SD	14.62 ± 23.88	23.44 ± 65.87	0.287
CD8[ad] (cell counts/mm^2)			
Mean ± SD	25.41 ± 35.22	15.01 ± 46.93	0.186
CD4/CD8[ad] (cell counts/mm^2)			
Mean ± SD	2.43 ± 10.06	4.09 ± 10.96	0.440
FOXP3[ad] (cell counts/mm^2)			
Mean ± SD	4.05 ± 10.46	9.61 ± 47.38	0.420
CD20[ad] (cell counts/mm^2)			
Mean ± SD	5.23 ± 11.30	5.20 ± 26.06	0.993
CD68[ad] (cell counts/mm^2)			
Mean±SD	60.76 ± 94.61	139.79 ± 185.12	0.002
CD163[ad] (cell counts/mm^2)			
Mean ± SD	234.18 ± 248.37	312.00 ± 325.30	0.155
CD163/CD68[ad] (cell counts/mm^2)			
Mean ± SD	12.80 ± 24.65	8.87 ± 18.01	0.307
AIF1[ad] (cell counts/mm^2)			
Mean ± SD	833.23 ± 383.28	834.92 ± 422.07	0.983
CD163/AIF1[ad] (cell counts/mm^2)			
Mean ± SD	0.45 ± 1.16	0.46 ± 0.41	0.936
IDO[ad]			
Mean ± SD	11.86 ± 12.96	1.40 ± 3.54	< 0.001

N number, *SD* standard deviation, *P P* value, *ST* supratentorial, *PF* posterior fossa, *SP* spinal

[a]These variables were compared using a Student's *t* test

[b]These variables were compared using a Chi square test

[c]These variables were compared using an ANOVA test

[d]These variables contain missing values that lacked information about the variables

respectively; Table 2). When the ratio of CD4+/CD8+ cells was included, except for in the case of CD8 + cell count, only a relatively low CD3+ cell number predicted a poor PFS ($P = 0.091$). When the numbers of CD3+, CD68+ and IDO+ cells were incorporated, immune cell subgroup B independently predicted an unfavorable PFS compared with immune cell subgroup A ($P < 0.001$; Table 3).

PD-L1 expression in ependymomas

PD-L1 expression was analyzed by two IHC clones, SP263 and E1L3N. Six (6/162, 3.7%) ependymoma cases positive for SP263 and three ependymoma (3/162, 1.9%) cases positive for E1L3N showed diffuse membranous expression of PD-L1 and extended to more than 50% of tumor cells (Fig. 4). All E1L3N-positive cases also expressed SP263.

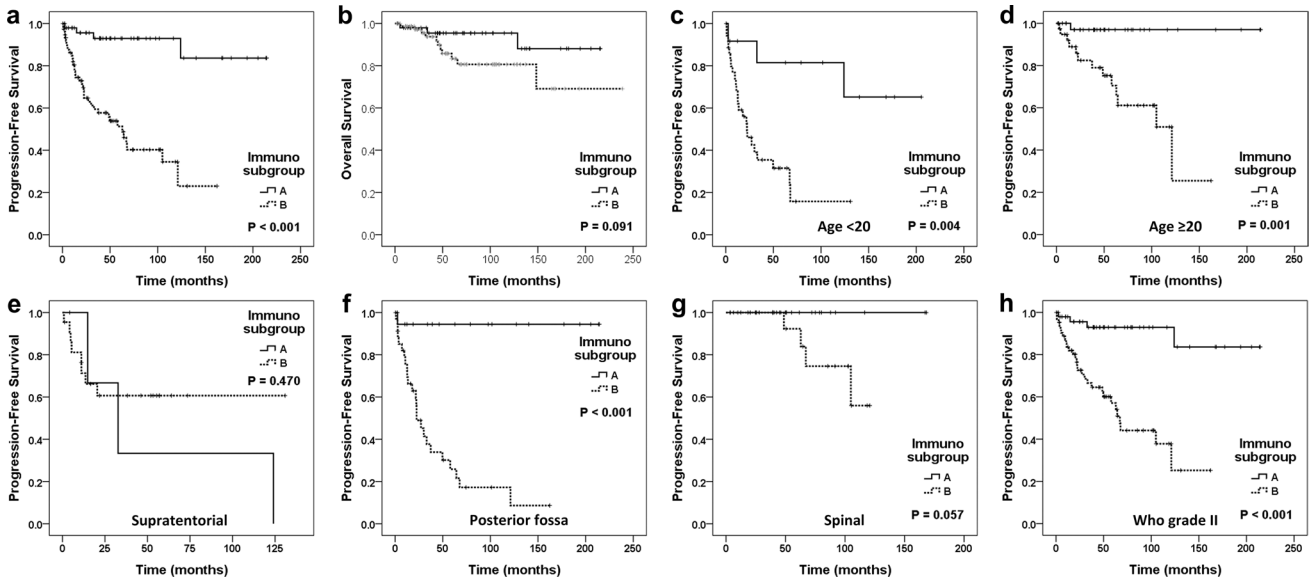

Fig. 3 Survival analysis according to the immune cell subgroups. Ependymoma patients were classified into two immune subgroups, immune cell subgroup A and B, using a k-means clustering analysis. Subgroup A was defined by high CD3+ and IDO+ cell counts and a low CD68+ cell count, and subgroup B was the opposite. The PFS and OS of ependymoma patients who were classified by WHO grade, age, and site of tumor were evaluated according to the immune cell subgroup. Kaplan–Meier curves for PFS and OS are illustrated with the P values from the log-rank test

All cases of both SP263 and E1L3N-positive ependymoma were WHO grade II, supratentorial, with high cytological atypia and positive L1CAM expression (Supplementary Table S3). In SP263-positive ependymoma cases, five PD-L1-positive ependymoma patients were pediatric (< 20), and another PD-L1-positive ependymoma patient was 39 years old. In E1L3N-positive ependymoma cases, all three cases of PD-L1 positive ependymomas were pediatric (age 9–13, mean 10.7). Among the L1CAM-positive cases with ST ependymomas, 40.0% (6/15) for SP263 and 20.0% (3/15) for E1L3N expressed membranous PD-L1.

The associations between PD-L1 (SP263) and the number of tumor-infiltrating immune cells are summarized in Supplementary Table S3. In PD-L1-positive ependymoma cases, the numbers of CD3+, CD4+, CD8+, FOXP3+, CD68+, and CD163+ cells were significantly increased compared with PD-L1-negative ependymoma cases ($P = 0.005$, 0.008, 0.032, 0.006, 0.003, and 0.002, respectively).

Patient survival analysis was performed according to PD-L1 expression. However, there was no statistical significance for PD-L1 expression in PFS or OS (data not shown).

Discussion

In the present study, we demonstrated that the amount of tumor-infiltrating immune cells affects the clinical outcome of patients with ependymoma. Briefly, increased numbers of CD3+ and CD8+ T-cells, a high ratio of CD4+/CD8+ cells and an increased number of IDO+ cells were associated with favorable prognosis, whereas increased numbers of FOXP3+ Tregs, CD68+ TAMs and a high ratio of CD163/AIF1+ cells indicating M2 polarization were associated with poor prognosis in ependymoma patients. In particular, patients in immune cell subgroup A, which were defined as having a combination of high CD3+ cells, low CD68+ and high IDO+ cells, showed a significantly prolonged survival.

The prognostic functions of the tumor-infiltrating immune cells were mostly consistent with the results of other studies on glioma. However, IDO+ cells exhibited a pattern that was different from those that were identified in other studies on glioma. In the present study, the counts of FOXP3 and IDO showed a significant positive correlation with each other. However, FOXP3 and IDO showed contrasting prognostic roles.

The paradoxical association of increased IDO+ cells with a favorable patient prognosis in ependymoma remains unclear. A study on gastric adenocarcinoma reported that high IDO was associated with better patient survival [28]. As a possible mechanism to explain their results, the authors suggested that higher stromal IDO could cause a decreased availability of tryptophan for tumor metabolism, thereby restricting the ability of the tumor to progress.

CD68 is a well-known marker for detecting cells in the monocyte lineage, including macrophages and microglia. AIF1, also known as ionized calcium-binding adapter molecule 1 (IBA1), is a specific marker for activated macrophages / microglia, especially in the CNS. The numbers of CD68+

Table 2 Multivariate analysis of PFS according to the clinicopathological parameters and tumor-infiltrating immune cells in ependymoma patients

Variables	HR (90% CI)	*P*
With CD8		
Age (< 20 vs ≥ 20)	1.355 (0.431–4.257)	0.603
KPS score (< 80 vs ≥ 80)	0.453 (0.172–1.195)	0.110
EOR (GTR vs STR)	5.652 (1.630-19.594)	0.006
Adjuvant radiotherapy (no vs yes)	1.048 (0.424–2.593)	0.918
Adjuvant chemotherapy (no vs yes)	1.143 (0.349–3.738)	0.825
WHO grade (II vs III)	0.555 (0.099–3.118)	0.504
Site (SP vs ST + PF)	0.275 (0.056–1.354)	0.112
MVP (absence vs presence)	3.268 (1.145–9.331)	0.027
Proliferating nodule (absence vs presence)	1.426 (0.541–3.761)	0.473
Atypia (low vs high)	1.123 (0.374–3.368)	0.837
Mitosis (< 5 vs ≥ 5)	1.297 (0.340–4.946)	0.703
CD3 (low vs high)	0.274 (0.067–1.123)	0.072
CD8 (low vs high)	0.407 (0.092–1.801)	0.236
FOXP3 (low vs high)	3.961 (1.441–10.885)	0.008
CD68 (low vs high)	5.587 (1.746–17.884)	0.004
CD163/AIF1 (low vs high)	3.160 (1.046–9.545)	0.041
IDO (low vs high)	0.183 (0.049–0.685)	0.012
With CD4/CD8		
Age (< 20 vs ≥ 20)	3.920 (0.738–20.836)	0.109
KPS score (< 80 vs ≥ 80)	0.602 (0.141–2.568)	0.493
EOR (GTR vs STR)	3.783 (1.052–13.605)	0.042
Adjuvant radiotherapy (no vs yes)	1.631 (0.449–5.924)	0.458
Adjuvant chemotherapy (no vs yes)	2.830 (0.571–14.018)	0.203
WHO grade (II vs III)	0.744 (0.066–8.446)	0.811
Site (SP vs ST + PF)	0.126 (0.016–0.982)	0.048
MVP (absence vs presence)	2.617 (0.650–10.540)	0.176
Proliferating nodule (absence vs presence)	1.464 (0.273–7.842)	0.656
Atypia (low vs high)	0.888 (0.168–4.709)	0.889
Mitosis (< 5 vs ≥ 5)	1.992 (0.254–15.625)	0.512
CD3 (low vs high)	0.306 (0.078–1.208)	0.091
CD4/CD8 (low vs high)	1.763 (0.403–7.711)	0.451
FOXP3 (low vs high)	2.384 (0.495–11.466)	0.278
CD68 (low vs high)	3.081 (0.713–13.313)	0.132
CD163/AIF1 (low vs high)	3.695 (0.732–18.656)	0.114
IDO (low vs high)	0.448 (0.121–1.662)	0.230

The quantities of immune cells were compared as categorical variables according to the cutoff values that were used for the Kaplan–Meier analysis and were subjected to univariate survival analyses using the Cox proportional hazard model

HR hazard ratio, *CI* confidence interval, *P P* value, *KPS score* Karnofsky Performance Status score, *EOR* extent of resection, *GTR* gross total resection, *STR* subtotal resection, *CT* chemotherapy, *RT* radiotherapy, *ST* supratentorial, *PF* posterior fossa, *SP* spinal, *MVP* microvascular proliferation

and AIF1+ cells were well correlated with each other, and the mean count of AIF1+ cells was five times higher than that of CD68+ cells (AIF1, 815.53 (range 56–1758, median 804.76) and CD68, 141.0 (range 0–1107.8, median 54.3) per 1 mm^2). Although CD68 and AIF1 are commonly used as markers for macrophages, their prognostic significance in ependymoma patients was quite different. While an increase in CD68+ TAMs was a statistically significant poor prognostic factor, AIF1+ TAM had no statistical significance but had a tendency to prolong survival (Fig. 2g, j). In another study, similar to our study, the number of AIF1+ TAMs was decreased in the patients who subsequently experienced recurrence [25]. However, in this study, CD68 + TMAs showed no statistically significant differences between non-recurrent and recurrent cases [25].

Ratios of CD163/CD68+ cells and CD163/AIF1+ cells, indicating M2 polarization, also showed different prognostic significance. While a high ratio of CD163/AIF1+ cells was a statistically significant poor prognostic factor in ependymoma patients, a high ratio of CD163/CD68+ cells showed an opposite tendency (Fig. 2k, i). These various results are because immune cell analysis was performed in a single antibody immunohistochemical staining. A variety of macrophage markers performing complex immunologic roles have been used in combination for detecting macrophages and represent several macrophage subsets, such as M1 and M2. Double or multiplex immunohistochemical staining can be helpful for more elaborate analysis of immune cells.

Genomic and transcriptomic studies have recently defined the distinct molecular subgroups of ependymoma that occur in three anatomic compartments of the central nervous system (supratentorial region, posterior fossa and spinal cord). Nine molecular subgroups were identified in a large cohort of ependymoma patients, with 3 subgroups in each anatomical compartment: the supratentorial region, posterior fossa and spinal cord [5, 29–31]. Except for the WHO grade I tumors, including the subependymomas and myxopapillary ependymomas at each site, there are two molecular subgroups in the ST region, two molecular subgroups in the PF, and one molecular subgroup in SP ependymomas.

Two ST subgroups were characterized based on the presence of prototypic fusion genes involving RELA and YAP1. Both the RELA-C11orf95 and YAP1-MAMLD1 fusions were further confirmed by a DNA methylation study. These mutations are mutually exclusive in ST ependymomas. The ST-RELA subgroup may occur in both children and adults and shows a dismal patient outcome. The YAP1 fusion-positive subgroup of ST ependymoma is enriched in the pediatric population and shows an excellent prognosis [5, 29, 32, 33].

Several transcriptional profiling studies of ependymomas, including both WHO grade II and III cases, revealed two genetically and clinically distinct subgroups of PF ependymomas, named group A (PF-A) and group B (PF-B). PF-A

Table 3 Multivariate analysis of PFS according to the clinicopathological parameters and combined TIL, TAM, and IDO status in ependymoma patients

Variables	HR (90% CI)	*P*
Age (< 20 vs ≥ 20)	0.682 (0.269–1.729)	0.420
KPS score (< 80 vs ≥ 80)	0.420 (0.194–0.908)	0.027
EOR (GTR vs STR)	2.644 (1.093–6.392)	0.031
Adjuvant radiotherapy (no vs yes)	0.838 (0.367–1.913)	0.674
Adjuvant chemotherapy (no vs yes)	1.643 (0.631–4.278)	0.309
WHO grade (II vs III)	3.617 (1.113–11.752)	0.032
Site (SP vs ST + PF)	2.876 (0.787–10.514)	0.110
MVP (absence vs presence)	2.017 (0.874–4.654)	0.100
Proliferating nodule (absence vs presence)	1.726 (0.718–4.146)	0.222
Atypia (low vs high)	1.034 (0.386–2.770)	0.947
Mitosis (< 5 vs ≥ 5)	0.553 (0.200-1.532)	0.255
Immune cell subgroup (A vs B)	15.049 (3.946–57.389)	< 0.001

The quantities of immune cells were compared as categorical variables according to the cutoff values that were used for the Kaplan–Meier analysis and were subjected to univariate survival analyses using the Cox proportional hazard model

HR hazard ratio, *CI* confidence interval, *P P* value, *KPS score* Karnofsky Performance Status score, *EOR* extent of resection, *GTR* gross total resection, *STR* subtotal resection, *CT* chemotherapy, *RT* radiotherapy, *ST* supratentorial, *PF* posterior fossa, *SP* spinal, *MVP* microvascular proliferation

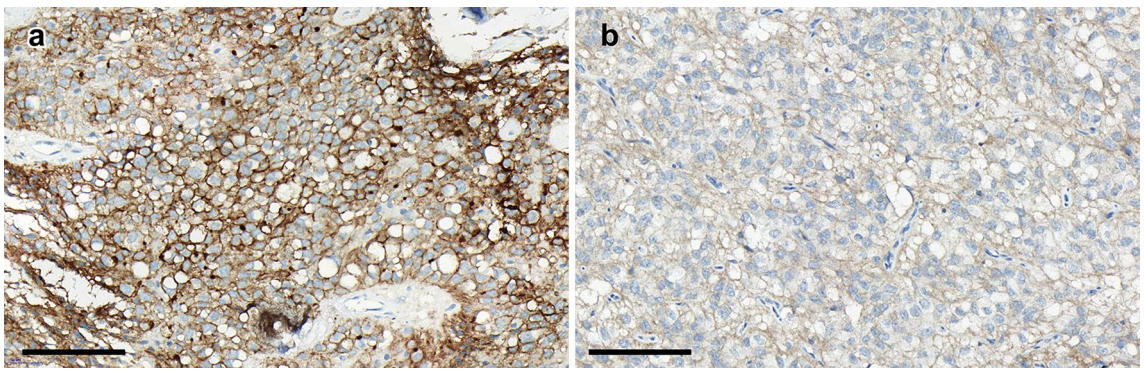

Fig. 4 Representative images of PD-L1 (SP263) strongly positive (**a**) and weakly positive (**b**) cases. PD-L1 positive ependymomas showed diffuse membranous patterns

predominantly occurs in infants and young children. PF-A is laterally located in the posterior fossa, has a balanced genome and is associated with a poor clinical prognosis. Conversely, PF-B largely occurs in adolescents and young adults and is associated with chromosomal instability and a more favorable prognosis [5, 33–36].

SP ependymomas constitute a molecularly distinct tumor group. They are a major disease component of neurofibromatosis type 2 (NF2) and are characterized by a high incidence of LOH on chromosome 22q, indicating the potential role of the NF2 gene in ependymomas with a spinal cord location. There have been studies showing the increased frequency of the NF2 gene mutation in these ependymomas [37, 38].

Among these molecular subgroups, the inflammatory response was identified as a molecular signature of high-risk PF-A ependymomas [35]. Griesinger et al. reported that the enrichment of IL6 and STAT3 pathway genes distinguished PF-A from PF-B and other brain tumors and resulted in myeloid polarization. Polarized myeloid cells drove unpolarized myeloid cells to upregulate CD163 and produce several proinflammatory cytokines. Therefore, the authors proposed that IL6/STAT3 pathway activation is critical in driving tumor growth and inflammatory crosstalk with myeloid cells within the PF-A microenvironment [39].

In the present study, unfortunately, we could not verify the molecular subgroups of the cohorts. Therefore, there is a limited ability to compare tumor-infiltrating immune cell expression to the molecular subgroup. However, in the present study, there was no prognostic implication of CD163 across all ependymoma patients or within PF ependymoma patients specifically (data not shown). Additionally, ratios of CD163/AIF1+ cells indicating M2 polarization showed

no prognostic implication in PF ependymoma patients. Studies have shown that tumor-infiltrating immune cells are influenced by numerous factors. Therefore, it is difficult to generalize the relationships between the molecular subtype and the tumor-infiltrating immune cell status within an ependymoma.

Higher grade of glioma had a tendency of more impaired humoral and cellular immunity against glioma genesis [40]. T lymphocytes can recognize tumor antigens. Immune checkpoints, particularly those involving PD-1 receptor and PD-L1, have several distinct mechanisms that can be responsible for T-cell dysfunction [41]. PD-1 and PD-L1 interaction induces the exhaustion and apoptosis of pathogen-specific T cells, and PD-1 blockade was able to restore function to these exhausted T cells [42]. Recently, immunotherapy targeting PD-1 and PD-L1 has evolved and produced significant positive results. The ongoing advances in successful immunotherapy for various cancers and the understanding of the tumor immune system have led to increased trials of PD-1 / PD-L1 inhibitors in the treatment of gliomas [6].

In the present study, only a small number of ependymoma cases expressed PD-L1. Although the prevalence of PD-L1-expressing ependymoma cases was too low to evaluate the clinicopathological significance of PD-L1, these cases were frequently observed in children and were found to have a low WHO grade, supratentorial location and positive L1CAM expression, suggesting a possible classification of ST-RELA. PD-L1-expressing ependymomas were associated with increased numbers of tumor-infiltrating immune cells. However, there was no prognostic significance for PD-L1 expression. Therefore, we proposed that there is a correlation between PD-L1 expression and ST-RELA. In another study, the authors found that the presence of ST-RELA suggested tumor evasion and immunosuppression due to PD-L1/PD-1-mediated T-cell exhaustion [9]. Overall, PD-L1 may be a potential immunotherapeutic target for ST-RELA patients.

Additionally, survival differences according to clinicopathologic features were analyzed in ependymoma patients. As in the preceding studies, younger age, low KPS score, suboptimal tumor resection, higher WHO grade and intracranial location were associated with poor prognosis [1]. Interestingly, both adjuvant radiotherapy and chemotherapy showed poor survival outcomes. These results are biased because in our cohort, adjuvant radiation therapy and chemotherapy tended to be administered in patients with high-risk factors such as young age, low KPS score, suboptimal tumor resection, high WHO grade, and intracranial location.

Several histopathologic features supporting WHO grade III anaplastic ependymoma noted in the 2016 WHO classification, including atypia, frequent mitotic figure, microvascular proliferation and necrosis, suggested poor prognosis. In addition, nodular proliferation was associated with the most significant worsening of outcome among all histopathologic features investigated. Nodular proliferation has been mentioned as a main factor in grading schemes in other studies [43]. Therefore, we propose that nodular proliferation can be considered one of the major high-grade features in ependymoma.

There are some limitations to this study. First, we could not identify the molecular subgroups of the samples. Molecular subclassification is expected to significantly support treatment decisions and should impact clinical trial design and operation in ependymoma patients [33]. We performed immunohistochemical staining for only L1CAM as a marker of ST-RELA. However, in the cohort in the present study, there was no significant prognostic difference between L1CAM-positive ST ependymoma and L1CAM-negative ST ependymoma, in contrast to previous reports [5].

Second, this study was a retrospective analysis. Therefore, the clinical features of patients varied. However, we verified that the prognostic tendency of immune cells was preserved in subgroup analysis according to age and site.

Third, the prognostic significance of immune cells was mainly found for PFS and not for OS, meaning that this analysis may have limited value in prognosis.

Fourth, we evaluated immune cell microenvironments under TMA. We validated our results using a subset of whole sections from reference cases. However, ICCs and P values between TMA and whole slide image of CD20 were insufficient for verifying representativeness. A possible cause is that there were too few CD20+ cells. Additionally, FOXP3 and IDO, with the second and third fewest numbers among immune cells, also had borderline ICC values. If the numbers of immune cells were not sufficiently large, the TMA method should be used with care.

However, the present study has some additional merits as follows: a relatively large number of patients were included, automatic cell counting was applied rather than manual evaluation, and the diverse tumor-infiltrating immune cells were analyzed together. Notably, CD3+ T cells and high CD3+ cell counts combined with low CD68+ and high IDO+ cell counts were strong and independent prognostic indicators.

In summary, increased numbers of CD3+, CD8+ and IDO+ cells decreased the number of $FOXP3^+$ cells, and high numbers of CD3+ cells in combination with low numbers of CD68+ cells are favorable independent prognostic factors for patients with ependymoma. An evaluation of the combined status of TILs, TAMs, and IDO+ cells may be beneficial for the risk stratification of patients with ependymoma. This study also provides valuable information for developing therapeutic strategies targeting the tumor microenvironment in patients with ependymoma.

Author contributions Study conception and design were performed by SJN and COS. SJN, COS, and SKK reviewed the pathological materials

according to current WHO criteria. SJN, Y-HK, and JEP reviewed and obtained detailed clinical data. Y-sR organized cohort of pediatric ependymoma patients and obtained clinical data from the medical records. YHC, and JHK organized cohort of adult ependymoma patients and obtained clinical data from the medical records. Statistical analysis was performed by SJN and COS. SJN prepared the initial manuscript. All co-authors made substantial contributions to the rewriting of the manuscript, review, and approval.

Compliance with ethical standards

Conflict of interest The authors declare that they have no conflict of interest.

Ethical approval and ethical standards. This study was performed with archived paraffin-embedded tissue samples. This study was approved by the Asan Medical Center Institutional review board (approval number 2016 – 1197) and was conducted in accordance with the Declaration of Helsinki.\

Informed consent Informed consent by individual patients could not be given, as the study only included paraffin-embedded archived tissue. With the approval of the ethical committee, informed consent was not required because all patient data were anonymized.

References

1. Kim YJ, Kim JY, Lim do H et al (2013) Retrospective analysis of treatment outcome of pediatric ependymomas in Korea: analysis of Korean multi-institutional data. J Neurooncol 113:39–48. https://doi.org/10.1007/s11060-013-1087-5
2. Nuno M, Yu JJ, Varshneya K et al (2016) Treatment and survival of supratentorial and posterior fossa ependymomas in adults. J Clin Neurosci 28:24–30. https://doi.org/10.1016/j.jocn.2015.11.014
3. Yang T, Wu L, Yang C, Deng X, Xu Y (2014) Clinical features and long-term outcomes of intraspinal ependymomas in pediatric patients. Child's Nerv Syst ChNS 30:2073–2081. https://doi.org/10.1007/s00381-014-2528-y
4. Louis DN, Ohgaki H, Wiestler OD, Cavenee WK (2016) WHO Classification of Tumours of the Central Nervous System, Revised. Fourth Edition. IARC WHO Classification of Tumours
5. Pajtler KW, Witt H, Sill M et al (2015) Molecular classification of ependymal tumors across all CNS compartments, histopathological grades, and age groups. Cancer Cell 27:728–743. https://doi.org/10.1016/j.ccell.2015.04.002
6. Xue S, Hu M, Iyer V, Yu J (2017) Blocking the PD-1/PD-L1 pathway in glioma: a potential new treatment strategy. J Hematol Oncol 10:81. https://doi.org/10.1186/s13045-017-0455-6
7. Srinivasan VM, Ferguson SD, Lee S et al (2017) Tumor vaccines for malignant gliomas. Neurotherapeutics 14:345–357. https://doi.org/10.1007/s13311-017-0522-2
8. Swartz MA, Iida N, Roberts EW et al (2012) Tumor microenvironment complexity: emerging roles in cancer therapy. Cancer Res 72:2473–2480. https://doi.org/10.1158/0008-5472.CAN-12-0122
9. Witt DA, Donson AM, Amani V et al (2018) Specific expression of PD-L1 in RELA-fusion supratentorial ependymoma: Implications for PD-1-targeted therapy. Pediatr Blood Cancer 65:e26960. https://doi.org/10.1002/pbc.26960
10. Kerkar SP, Restifo NP (2012) Cellular constituents of immune escape within the tumor microenvironment. Cancer Res 72:3125–3130. https://doi.org/10.1158/0008-5472.CAN-11-4094
11. Han S, Zhang C, Li Q et al (2014) Tumour-infiltrating CD4(+) and CD8(+) lymphocytes as predictors of clinical outcome in glioma. Br J Cancer 110:2560–2568. https://doi.org/10.1038/bjc.2014.162
12. Kmiecik J, Poli A, Brons NH et al (2013) Elevated CD3+ and CD8+ tumor-infiltrating immune cells correlate with prolonged survival in glioblastoma patients despite integrated immunosuppressive mechanisms in the tumor microenvironment and at the systemic level. J Neuroimmunol 264:71–83. https://doi.org/10.1016/j.jneuroim.2013.08.013
13. Sayour EJ, McLendon P, McLendon R et al (2015) Increased proportion of FoxP3+ regulatory T cells in tumor infiltrating lymphocytes is associated with tumor recurrence and reduced survival in patients with glioblastoma. Cancer Immunol Immunother 64:419–427. https://doi.org/10.1007/s00262-014-1651-7)
14. Yue Q, Zhang X, Ye H-x et al (2014) The prognostic value of Foxp3+ tumor-infiltrating lymphocytes in patients with glioblastoma. J Neurooncol 116:251–259. https://doi.org/10.1007/s11060-013-1314-0)
15. Domingues P, Gonzalez-Tablas M, Otero A et al (2016) Tumor infiltrating immune cells in gliomas and meningiomas. Brain Behav Immun 53:1–15. https://doi.org/10.1016/j.bbi.2015.07.019
16. Kennedy BC, Showers CR, Anderson DE et al (2013) Tumor-associated macrophages in glioma: friend or foe? J Oncol 2013:486912. https://doi.org/10.1155/2013/486912
17. Ye XZ, Xu SL, Xin YH et al (2012) Tumor-associated microglia/macrophages enhance the invasion of glioma stem-like cells via TGF-beta1 signaling pathway. J Immunol 189:444–453. https://doi.org/10.4049/jimmunol.1103248
18. Munn DH, Mellor AL (2013) Indoleamine 2,3 dioxygenase and metabolic control of immune responses. Trends Immunol 34:137–143. https://doi.org/10.1016/j.it.2012.10.001
19. Wilke CM, Zou W (2011) T lymphocytes to IDO+ cells: check. Blood 117:2082–2083. https://doi.org/10.1182/blood-2010-12-322172
20. Godin-Ethier J, Hanafi LA, Piccirillo CA, Lapointe R (2011) Indoleamine 2,3-dioxygenase expression in human cancers: clinical and immunologic perspectives. Clin Cancer Res 17:6985–6991. https://doi.org/10.1158/1078-0432.CCR-11-1331
21. Zhai L, Ladomersky E, Lauing KL et al (2017) Infiltrating T cells increase ido1 expression in glioblastoma and contribute to decreased patient survival. Clin Cancer Res 23:6650–6660. https://doi.org/10.1158/1078-0432.CCR-17-0120
22. Wainwright DA, Chang AL, Dey M et al (2014) Durable therapeutic efficacy utilizing combinatorial blockade against IDO, CTLA-4, and PD-L1 in mice with brain tumors. Clin Cancer Res 20:5290–5301. https://doi.org/10.1158/1078-0432.CCR-14-0514
23. Wainwright DA, Balyasnikova IV, Chang AL et al (2012) IDO expression in brain tumors increases the recruitment of regulatory T cells and negatively impacts survival. Clin Cancer Res 18:6110–6121. https://doi.org/10.1158/1078-0432.CCR-12-2130
24. Wainwright DA, Dey M, Chang A, Lesniak MS (2013) Targeting tregs in malignant brain cancer: overcoming IDO. Front Immunol 4:116. https://doi.org/10.3389/fimmu.2013.00116
25. Donson AM, Birks DK, Barton VN et al (2009) Immune gene and cell enrichment is associated with a good prognosis in ependymoma. J Immunol 183:7428–7440. https://doi.org/10.4049/jimmunol.0902811
26. Nam SJ, Go H, Paik JH et al (2014) An increase of M2 macrophages predicts poor prognosis in patients with diffuse large B-cell lymphoma treated with rituximab, cyclophosphamide, doxorubicin, vincristine and prednisone. Leukemia Lymphoma 55:2466–2476. https://doi.org/10.3109/10428194.2013.879713
27. Budczies J, Klauschen F, Sinn BV et al (2012) Cutoff Finder: a comprehensive and straightforward web application enabling rapid biomarker cutoff optimization. PLoS One 7:e51862. https://doi.org/10.1371/journal.pone.0051862

28. Patil PA, Blakely AM, Lombardo KA et al (2018) Expression of PD-L1, indoleamine 2,3-dioxygenase and the immune microenvironment in gastric adenocarcinoma. Histopathology. https://doi.org/10.1111/his.13504 **(epub ahead of print)**
29. Parker M, Mohankumar KM, Punchihewa C et al (2014) C11orf95-RELA fusions drive oncogenic NF-kappaB signalling in ependymoma. Nature 506:451–455. https://doi.org/10.1038/nature13109
30. Witt H, Mack SC, Ryzhova M et al (2011) Delineation of two clinically and molecularly distinct subgroups of posterior fossa ependymoma. Cancer Cell 20:143–157. https://doi.org/10.1016/j.ccr.2011.07.007
31. Mack SC, Witt H, Piro RM et al (2014) Epigenomic alterations define lethal CIMP-positive ependymomas of infancy. Nature 506:445–450. https://doi.org/10.1038/nature13108
32. Gupta K, Salunke P (2015) Understanding ependymoma oncogenesis: an update on recent molecular advances and current perspectives. Mol Neurobiol 54:15–21. https://doi.org/10.1007/s12035-015-9646-8
33. Pajtler KW, Mack SC, Ramaswamy V et al (2017) The current consensus on the clinical management of intracranial ependymoma and its distinct molecular variants. Acta Neuropathol 133:5–12. https://doi.org/10.1007/s00401-016-1643-0
34. Thompson YY, Ramaswamy V, Diamandis P, Daniels C, Taylor MD (2015) Posterior fossa ependymoma: current insights. Child's Nerv Syst ChNS. 31:1699–1706. https://doi.org/10.1007/s00381-015-2823-2
35. Wani K, Armstrong TS, Vera-Bolanos E et al (2012) A prognostic gene expression signature in infratentorial ependymoma. Acta Neuropathol 123:727–738. https://doi.org/10.1007/s00401-012-0941-4
36. Archer TC, Pomeroy SL (2011) Posterior fossa ependymomas: a tale of two subtypes. Cancer Cell 20:133–134. https://doi.org/10.1016/j.ccr.2011.08.003
37. Ebert C, von Haken M, Meyer-Puttlitz B et al (1999) Molecular genetic analysis of ependymal tumors. Am J Pathol 155:627–632. https://doi.org/10.1016/s0002-9440(10)65158-9
38. Korshunov A, Neben K, Wrobel G et al (2003) Gene expression patterns in ependymomas correlate with tumor location, grade, and patient age. Am J Pathol 163:1721–1727. https://doi.org/10.1016/s0002-9440(10)63530-4
39. Griesinger AM, Josephson RJ, Donson AM et al (2015) Interleukin-6/STAT3 pathway signaling drives an inflammatory phenotype in group A ependymoma. Cancer Immunol Res 3:1165–1174. https://doi.org/10.1158/2326-6066.CIR-15-0061
40. Gousias K, Markou M, Arzoglou V et al (2010) Frequent abnormalities of the immune system in gliomas and correlation with the WHO grading system of malignancy. J Neuroimmunol 226:136–142. https://doi.org/10.1016/j.jneuroim.2010.05.027
41. Sanmamed MF, Chen L (2014) Inducible expression of B7-H1 (PD-L1) and its selective role in tumor site immune modulation. Cancer J 20:256–261. https://doi.org/10.1097/PPO.0000000000000061
42. Wei F, Zhong S, Mae Z et al (2013) Strength of PD-1 signaling differentially affects T-cell effector functions. Proc Natl Acad Sci USA 110:10892. https://doi.org/10.1073/pnas.1305394110
43. Ellison DW, Kocak M, Figarella-Branger D et al (2011) Histopathological grading of pediatric ependymoma: reproducibility and clinical relevance in European trial cohorts. J Negat Results Biomed 10:7. https://doi.org/10.1186/1477-5751-10-7